INSTITUT FRANCO-ALLEMAND DE RECHERCHES DE SAINT-LOUIS
DEUTSCH-FRANZÖSISCHES FORSCHUNGSINSTITUT SAINT-LOUIS

5 rue du Général Cassagnou - 68301 Saint-Louis - France

Tél. +33 (0)3 89 69 50 00 - Fax +33 (0)3 89 69 50 00
http://www.isl.tm.fr

Adresse postale : BP 70034 - 68301 SAINT LOUIS CEDEX - France
Postanschrift: Postfach 1260 - 79574 Weil am Rhein - Deutschland

Elaboration and Characterization of Nano-Sized $Al_xMo_yO_z$/Al Thermites

COMET M., SPITZER D.

IPS2006, 33rd International Pyrotechnics Seminar,
Fort Collins/CO, US, July 16-21, 2006

PU 614/2006

Axe de recherches
Schwerpunkt **2.11**

REPORT DOCUMENTATION PAGE

Form Approved OMB No. 0704-0188

1. AGENCY USE ONLY (Leave blank)	2. REPORT DATE	3. REPORT TYPE AND DATES COVERED
	July 2006	Seminar Paper

4. TITLE AND SUBTITLE

Elaboration and Characterization of Nano-Sized Al_x,Mo_yO_z/ Al Thermites

5. FUNDING NUMBERS

6. AUTHOR(S)

M. Comet, D. Spitzer

7. PERFORMING ORGANIZATION NAME(S) AND ADDRESS(ES)

Institut franco-allemand de recherches de Saint Louis, 68300 Saint Louis, France

9. SPONSORING/MONITORING AGENCY NAME(S) AND ADDRESS(ES

Institut franco-allemand de recherches de Saint Louis, 68300 Saint Louis, France

10. SPONSORING/MONITORING AGENCY REPORT NUMBER

PU 614/2006

11. SUPPLEMENTARY NOTES

Text in English, 10 pages, 8 references, 4 tables. Presented at the IPS2006, 33rd International Pyrotechnics Seminar, in Fort Collins, Colorado, 16-21 July 2006.

12a. DISTRIBUTION/AVAILABILITY STATEMENT

12b. DISTRIBUTION CODE

ABSTRACT (Maximum 200 words)

A new process to control the reactivity of thermites containing molybdenum trioxide (MoO_3) and aluminium (Al) has been developed at the Institut franco-allemand de recherches de Saint Louis (ISL). This process consists to elaborate by a new sol-gel method nano-sized mixed Al_x,Mo_yO_z phases whose structure is correlated to the chemical composition. It is so possible to adjust the energetic properties of the thermites obtained through physical mix of these phases with nano-sized aluminium (Al 50-P, Nanotechnologies). The resulting nanothermites are very insensitive to mechanical and thermal stresses, but can be easily ignited by the energy brought by a laser beam. The nano-structuring of the oxidative phase decreases the sensitivities, shortens the ignition delay times and dramatically increases the combustion rates. These promising characteristics allow considering these metastable interstitial composites (MICs) as potential components for insensitive weapon ignition systems.

14. SUBJECT TERMS

ISL, German, Thermites, Molybdenum trioxide, Aluminium, Nanotechnology, Nanothermites, Thermal stress, Combustion rates, Metastable interstitial composites, Weapon ignition systems

15. NUMBER OF PAGES

16. PRICE CODE

17. SECURITY CLASSIFICATION OF REPORT	18. SECURITY CLASSIFICATION OF THIS PAGE	19, SECURITY CLASSIFICATION OF ABSTRACT	20. LIMITATION OF ABSTRACT
UNCLASSIFIED	UNCLASSIFIED	UNCLASSIFIED	UL

Elaboration and characterization of nano-sized $Al_xMo_yO_z$ / Al thermites

M. Comet, D. Spitzer
Institut franco-allemand de recherches de Saint Louis, 68300 Saint Louis, France

ABSTRACT

A new process to control the reactivity of thermites containing molybdenum trioxide (MoO_3) and aluminium (Al) has been developed at the Institut franco-allemand de recherches de Saint Louis (ISL). This process consists to elaborate by a new sol-gel method nano-sized mixed $Al_xMo_yO_z$ phases whose structure is correlated to the chemical composition. It is so possible to adjust the energetic properties of the thermites obtained through physical mix of these phases with nano-sized aluminium (Al 50-P, Nanotechnologies). The resulting nanothermites are very insensitive to mechanical and thermal stresses, but can be easily ignited by the energy brought by a laser beam. The nano-structuring of the oxidative phase decreases the sensitivities, shortens the ignition delay times and dramatically increases the combustion rates. These promising characteristics allow considering these metastable interstitial composites (MICs) as potential components for insensitive weapon ignition systems.

INTRODUCTION

The effect of the aluminium particles sizes on the reactivity of thermites composed of molybdenum trioxide (MoO_3) and aluminium was recently studied by several authors. It was reported that materials in which aluminium is structured at the nano-scale have thermal sensitivity two magnitudes higher than their micron-size counterparts[1] and a dramatically increased combustion rate[2]. The idea developed at the Institut franco-allemand de recherches de Saint Louis (ISL) is to control the reactivity of such thermites through the composition and the structure of the molybdenum oxide.

To this purpose an unconventional method branching of the sol-gel process was set up to elaborate nano-sized $Al_xMo_yO_z$ phases. The ratio of aluminium to molybdenum in the $Al_xMo_yO_z$ phase is used to control the structure and the reactivity of $Al_xMo_yO_z$ / Al based thermites.

1. Synthesis of the nano-sized $Al_xMo_yO_z$ oxidative phases

1-1. Elaboration of agar based composite gels

Agar is a galactose polymer obtained from the cell walls of some species of red algae or seaweed. When dissolved in hot water and cooled, agar gives gels which are more and more substantial than the ratio agar : water becomes higher. The gelling properties of agar in aqueous media are widely used in biology to grow bacteria and fungi. But to our knowledge, the use of this compound as a structuring agent in materials science was never reported before the recent paper of Kawano et al.[3]. This process however consists in precipitating zinc hydroxide from Zn^{2+} ions contained within the agar gel. So, although the agar was used by these authors as a structuring agent, their method considerably differs from the one described herein.

The composite agar based gels used in this study were elaborated as follows:
A solution of 40.46 $mmol.L^{-1}$ (about 50 $g.L^{-1}$) is prepared by dissolving ammonium paramolybdate (APM, $H_{24}Mo_7N_6O_{24} \cdot 4H_2O$, $\geq 99.0\%$; Fluka) into deionised water. To various amounts of agar powder (Merck, fire ash < 3%) was added a given volume of the APM solution. The suspensions are heated using a hot plate at temperatures ranging from 333 to 343 K in order to dissolve agar and to obtain clear solutions. The concentration of agar in the APM solution ranges typically from 0.85 to 15 % w/v. The gelling is induced by spontaneous cooling of the solutions at room temperature ($T \approx 293$ K). The water is extracted from the gel by washing it with acetone in a Soxhlet apparatus during approximately a hundred of

AQ F07-01-0196

cycles (2 to 4 min per cycle). The acetone mixes with water and induces the co-precipitation of the agar and the APM. The residual acetone is evaporated in a vacuum drying oven at room temperature. The final material is composed of hollow monoliths, even more crumbly than there is less agar. The composite APM / agar gel is ground into liquid nitrogen in order to have a powder easy to handle and to characterize. If the grinding step is performed at room temperature, the material undergoes decomposition: the initial white slight pale-blue coloration turns then black.

Pure agar gels used as references were elaborated following the same experimental protocol. The APM aqueous solution is then replaced by deionised water. As these materials were very hard, they were not ground but pulverized using a diamond file.

In the following text, the pure agar gels and the composite gels (CG) will be labelled by the masses and the volume of each reagent used to make them: agar (g) : APM (g) : solution (mL).

1-2. Structural characterization of agar based composite gels

First, the structure of pure agar gels was compared to the one of the composite gels by scanning electron microscopy (**Figure 1a, 1b**). The micrographs were taken at the same magnification (x 10,000) to give a global view of the structure of the two samples, but the quantitative measurements were done at higher magnification (50,000 to 100,000). The APM and agar composite gels have a three-dimensional porous structure formed of interlinked strands of average section equal to 45 nm ($20 < \Phi < 90$ nm, **Figure 1a**), whereas pure agar-containing gels are not structured at the nano-scale and do not exhibit porosity (**Figure 1b**). The structure appearance of composite gels is reminiscent of the nerve-cells one. This structure, which is systematically observed on this kind of material, is due to the agar and APM co-precipitation during the water extraction with acetone. Micron-sized free particles were here and there observed in poor agar-containing composite gels (agar content below 23 w%). These particles form outside the gel during the extraction of water by acetone. This phenomenon called "exocrystallization" is even more obvious than the proportion of agar to APM is low. The same phenomenon has been observed when the proportion of agar to water is lowered. "Exocrystallization" of APM does not occur in the richest agar-containing gels. The fact that a single phase is observed shows that the material is a nano-sized composite in which the APM particles are necessarily smaller than the strands that they are part of. Transmission electron microscopy observations confirm that the composite gels have an interconnected fibrous structure (**Figure 1c**). APM particles have an isotropic sphere-like shape and are located along agar strands defining a stringer-like structure.

The electron microscopy qualitative observations were quantitatively confirmed by nitrogen adsorption (BET method) which showed that the specific surface area of pure agar gel does not exceed some square meters per gram whereas it ranges from 26 to 116 $m^2.g^{-1}$ in the case of the composite gels (**Table 1**). The value of the surface area is a good criterion to know if a given material is structured at the nano-scale insofar as it gives more global information on a sample than the microscopy does.

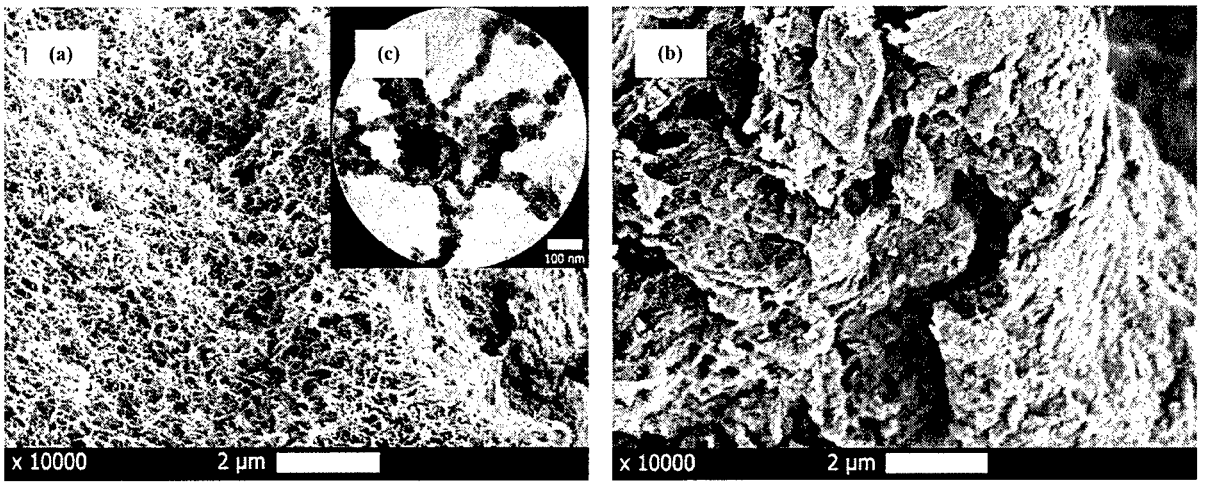

Figure 1: SEM micrographs of a 40 w% agar-containing composite gel **(a)** and of a pure agar gel **(b)**. TEM micrograph of a 68 w% agar-containing composite gel **(c)**.

To calculate the average size of the APM particles using the measures of the surface area, a model in good agreement with the microscopic observations was set up (**Figure 1c**). Thus, the particles of APM are considered to be spheres contained in a non-porous cylinder of agar and separated from a distance which is assumed to be constant (**Figure 2**):

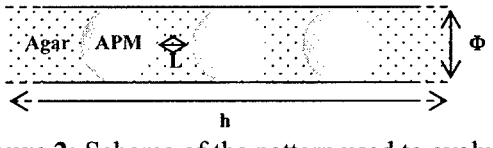

Figure 2: Scheme of the pattern used to evaluate the size of the APM nanoparticles (**Φ**) and the average distance which separates them (**L**).

The measured surface area is the ratio of the external geometric surface of the cylinder to its mass. It can be expressed as a function of Φ and L, using the respective densities of the APM ($\rho_{APM} \approx 2.8$) and of the agar ($\rho_A \approx 1.4$):

$$S_{BET} = \frac{2\pi\left(\frac{\Phi}{2}\right)h}{\rho_{APM}\frac{\pi h\Phi^3}{6(L+\Phi)} + \rho_A\left[\frac{\pi h\Phi^2}{4} - \frac{\pi h\Phi^3}{6(L+\Phi)}\right]}$$

Once simplified, it gives:

$$S_{BET} = \frac{12(L+\Phi)}{\Phi(2\rho_{PMA}\Phi + \rho_A\Phi + 3\rho_A L)} \qquad (1)$$

To obtain the second equation necessary to solve the system, the volume ratio of the APM ($\chi_{V/APM}$) was also expressed as a function of Φ and L, and calculated from the experiment with the APM and the agar weight ratios (respectively $\chi_{W/APM}$; $\chi_{W/A} = 1 - \chi_{W/APM}$):

$$\chi_{V/APM} = \frac{\frac{\pi\Phi^3 h}{6(L+\Phi)}}{\frac{\pi h\Phi^2}{4}} = \frac{2\Phi}{3(L+\Phi)} \qquad (2)$$

$$\chi_{V/APM} = \frac{\chi_{W/APM}\rho_A}{\chi_{W/APM}(\rho_A - \rho_{APM}) + \rho_{APM}}$$

The solving of the system defined by the equations (1) and (2) finally permits to express Φ and L from the experimental parameters S_{BET} and $\chi_{W/APM}$:

$$\Phi = \frac{4}{S_{BET}(\rho_{APM}\chi_{V/APM} + \rho_A(1-\chi_{V/APM}))}$$

$$L = \frac{4(2-3\chi_{V/APM})}{3S_{BET}\chi_{V/APM}(\rho_{APM}\chi_{V/APM} + \rho_A(1-\chi_{V/APM}))}$$

The surface areas (S_{BET}) are experimentally determined using nitrogen adsorption. To this purpose, the composite gels were first heated at 80°C in a helium flow during at least six hours in order to remove adsorption water which represents about 10% of the global weight of composite gels. The volume ratios of the APM

are deduced from the mass ratios found by using Thermogravimetric Analysis (TGA). From these values, the average size of the APM particles and the distance separating them were calculated (**Table 1**). The gels considered as the best precursors of the nano-sized $Al_xMo_yO_z$ phases are those with the smallest APM particles (Φ small) and the ones in which the APM particles are separated by the largest distance possible (L large). When the L value tends to zero, it means that the APM particles are in contact. This critical value is reached when a composite gel contains 79.8% in weight of APM. Outside this limit ($\chi_{W/APM} > 79.8\%$), the model previously described cannot be used any longer. Then, the APM particles nucleate and grow outside the agar strands. This is the "exocrystallisation" phenomenon which was experimentally observed by SEM on the APM richer compositions.

As a general rule, the more agar a composite gel contains, the higher is the surface area. However, when the proportion of agar to water becomes too important (e.g. composition 1.50 : 0.50 : 10), the agar is hardly dissolved and the surface area decreases. Moreover, the surface area of the composite gels gets higher as less water is added.

Pure agar gels elaborated within the same conditions than the composite gels are non porous and have a surface area which corresponds to the geometric surface of the agar particles. This statement is in good agreement with the results obtained by electron microscopy and shows that the very particular nano-sized structure of the composite gels is linked to the agar and APM interactions.

From a structural point of view, the best gels to elaborate nano-sized $Al_xMo_yO_z$ phases must contain 40 to 60 percents in weight of agar and must be elaborated with a weight to volume ratio of agar to APM solution ranging from 1 : 10 to 1 : 20.

Synthesis conditions Agar (g) : APM (g) : Solution (mL)	Actual composition Agar : APM (w%)	S_{BET} ($m^2.g^{-1}$)	Φ (nm)	L (nm)
0.17 : 0.50 : 10	15.4 : 84.6	25.7	-	-
0.21 : 0.50 : 10	18.7 : 81.3	29.3	-	-
0.25 : 0.50 : 10	23.3 : 76.7	35.6	50	1.2
0.50 : 0.50 : 10	40.5 : 59.5	76.4	27	2.8
1.00 : 0.50 : 10	60.0 : 40.0	116.3	20	2.0
1.50 : 0.50 : 10	68.6 : 31.4	108.1	22	2.0
0.25 : 0.50 : 20	24.8 : 75.2	29.7	60	2.1
0.50 : 0.50 : 20	41.5 : 58.5	59.3	34	3.5
1.00 : 0.50 : 20	59.5 : 40.5	82.2	28	2.9
1.50 : 0.50 : 20	73.0 : 27.0	99.2	25	2.0
1.50 : 0.00 : 20	100.0 : 0.0	3.2	-	-
0.50 : 0.00 : 20	100.0 : 0.0	4.3	-	-

Table 1: Values of BET-N_2 surface area of the composite gels as a function of their composition. These experimental values were used to evaluate the average diameter (Φ) of the APM particles embedded in agar strands and the mean distance between these particles (L).

1-3. Elaboration of the nano-sized $Al_xMo_yO_z$ phases

The experimental elaboration of the $Al_xMo_yO_z$ nano-sized phases from the composite gels is typically performed as follows: a 4.00 g sample of a 7.5 : 5.0 : 100 composite gel is weighted in a 500 mL one-neck round-bottom flask. The composite gel powder is impregnated by 60 mL of anhydrous aluminium trichloride ($AlCl_3$; Sigma-Aldrich; purity ≥ 99.9%; further noted AAT) solutions in diethyether (Et_2O; Aldrich; purity ≥ 99.7%). This solvent was chosen because of its good ability to dissolve AAT and its compatibility with both agar and APM. The concentrations of AAT were respectively equal to 15, 30 and 60 $g.L^{-1}$. The mixture is a flowing paste which is homogenised by applying ultrasounds at room temperature during one minute, using an ultrasonic bath. Diethylether is evaporated at 313 K under reduced pressure using a rotary evaporator. The impregnated materials are finally calcined into a programmable muffle furnace. The calcination is carried out under an air atmosphere, continuously renewed by a vacuum pump working in reverse order. The heating program used was a 10 $K.min^{-1}$ ramp from 303 K to 823 K followed by an isothermal treatment at 823 K applied during two hours. The samples were then allowed to cool and removed from the furnace at room temperature.

In order to have a reference material, a 4.00 g sample of a 7.5 : 5.0 : 100 composite gel was calcined without previous infiltration by an AAT solution.

1.4. Structural characterization of the nano-sized $Al_xMo_yO_z$ phases

The microstructure of the reference material obtained by direct calcination of the composite gel without a preliminary AAT infiltration leads to micron-sized molybdenum trioxide particles being roof tile-shaped like (**Figure 2a**). When the composite gel is impregnated with an AAT solution in diethylether before the calcination step, the resulting particles are far smaller (**Figure 2b, 2c, 2d**). Their sizes directly depend on the concentration of the AAT solution. These particles are sphere-like slightly elongated and keep a three dimensional organization reminding the one of the composite gels. This trend was corroborated by the values of the surface areas measured on these samples by gas adsorption. These results can be explained by the fact that the adsorbed water contained into the composite gel reacts with the AAT to form a thin layer of aluminium oxychloride at the surface of the gel strands. During the thermal treatment, this layer prevents the sintering, by acting as an in-situ nano-sized crucible. The major part of chlorine atoms is removed and several chemical species are formed leading to $Al_xMo_yO_z$ phases.

The nature of these phases was studied by X-rays diffraction which showed that they were composed of an amorphous part as well as nano-crystalline species. The non-crystallized phase is probably alumina or an aluminium oxychloride because the amorphous content is all the more important as the $Al_xMo_yO_z$ phase contains more aluminium. The crystallized species are the molybdenum dioxide (MoO_2) and the aluminium molybdate ($Al_2(MoO_4)_3$). In the case of the molybdenum dioxide, the size of elementary crystallites is constant ($\Phi \approx 70$ nm) whereas the size of the aluminium molybdate entities decreases when the aluminium content increases. The highest oxidation state of molybdenum (Mo^{+VI}) is stabilized by aluminium in the molybdate anion form, whereas the molybdenum (Mo^{+IV}) appears in the form of MoO_2. The under oxygenated MoO_2 phase probably forms in the reducing environment of the agar strand core. The aluminium molybdate most likely appears at the surface of the agar strand, where the APM particles are in contact with AAT and oxygen from air.

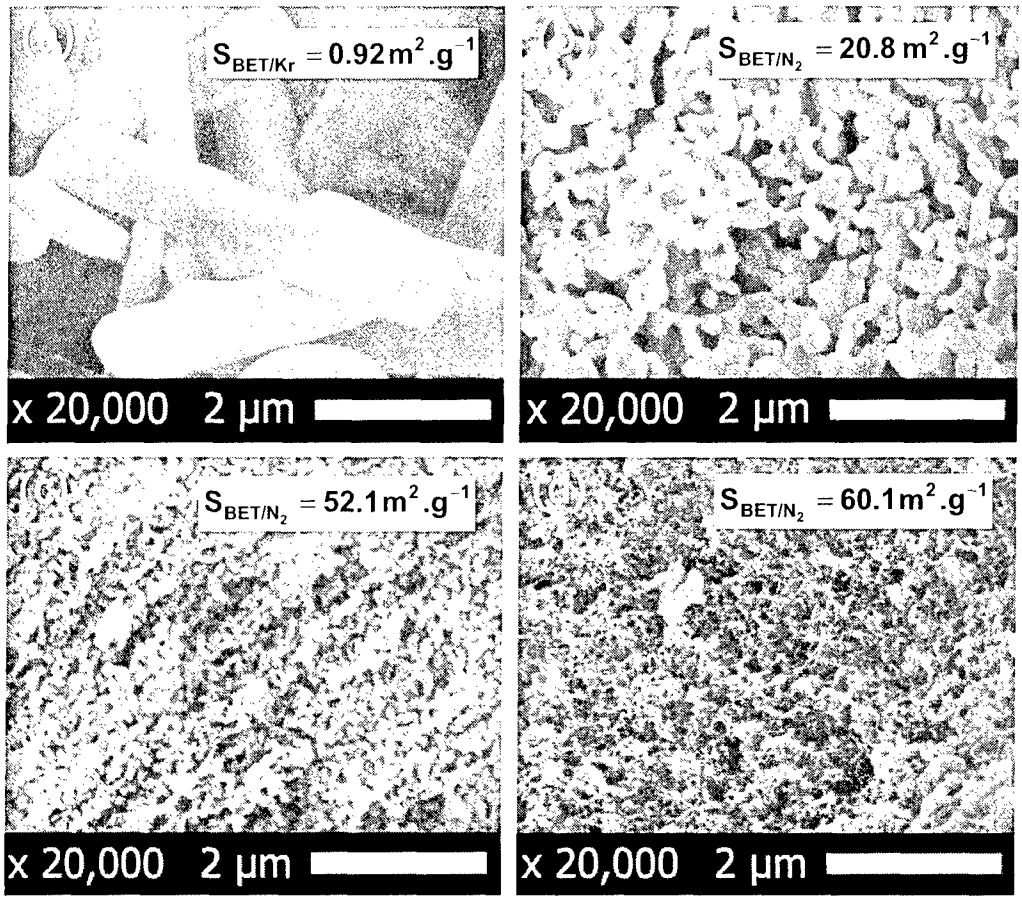

Figure 2: Characterization by scanning electron microscopy (SEM) and gas adsorption (BET) of particles formed by oxidation at 823 K of: a raw composite gel **(a)**, a composite gel impregnated with respectively 18.4 w% **(b)**, 31.0 w% **(c)** and 47.4 w% **(d)** of AAT.

2. $Al_xMo_yO_z$ / Al based nanothermites

2.1. Elaboration of $Al_xMo_yO_z$ / Al nanothermites

Nanothermites were elaborated by physical mix[4] of the $Al_xMo_yO_z$ nano-sized phases with aluminium nanoparticles. Nano-sized aluminium (Al 50-P) was purchased from Nanotechnologies and stored once opened in a moisture free atmosphere. In fact, a study by gas adsorption of Al 50-P aging has showed that this kind of aluminium is not too sensitive to severe storage conditions, except for the condensation of atmospheric moisture induced by sudden temperature changes. This observation seems to be in good agreement with the conclusions of Ramaswamy et al.[5] who assert that the water adsorbed into the alumina shell which covers the aluminium nanoparticles, plays a major role in the nano-aluminium aging process. The composition Al : Al_2O_3, the mean size of the particles, the diameter of the aluminium core and the thickness of the alumina shell were determined following the experimental method described by Pesiri et al.[6] The Al 50-P used to elaborate the nanothermites contains 66.6% by weight of metallic aluminium. The specific surface area being equal to 40.9 $m^2.g^{-1}$, the Al 50-P particles are composed of a 45.7 nm metallic aluminium core embedded in 2.9 nm thick alumina shell. The chemical composition of each $Al_xMo_yO_z$ phase was defined by quantitative elemental analysis (**Table 2**). The « useful » quantity of oxygen is deduced from these results, assuming that the only oxygen atoms which can react during the combustion of $Al_xMo_yO_z$ / Al nanothermites are those which are chemically linked to molybdenum. To this purpose, the global formula of the $Al_xMo_yO_z$ phases can be rewritten as follows $(Al_2O_3)_{0.5x}(MoO_{(z-1.5x)/y})$. The number of

pyrotechnically active oxygen atoms is noted u (u = (z-1.5x)/3y). This value which ranges from 2 to 3 is used to write the stoichiometric equation of the combustion:

$MoO_u + (2u/3)\ Al \rightarrow Mo + (u/3)\ Al_2O_3$

According to Pantoya et al.[1] the best energetic performances for the MoO_3 / Al based thermites ignited in ambient atmosphere are obtained with a slight excess of aluminium (+ 20% in weight) in comparison with the theoretical stoichiometry. The experimental proportions of $Al_xMo_yO_z$ nano-sized phases to Al 50-P were calculated from the elemental analysis results (**Table 2**).

Elaboration CG : AAT (g)	Mo (w%)	Al (w%)	O (w%)	Cl (w%)	Phases formulae	Composition (w%) $Al_xMo_yO_z$: Al 50-P	Index
4.00 : 0.00	66.7	0.0	33.3	-	MoO_3	59.7 : 40.3	Th.1
4.00 : 0.90	50.0	10.5	33.2	6.3	$(Al_2O_3)_{0.19}(MoO_{2.85})$	65.0 : 35.0	Th.2
4.00 : 1.80	41.0	16.8	32.3	9.9	$(Al_2O_3)_{0.31}(MoO_{2.54})$	69.4 : 30.6	Th.3
4.00 : 3.60	30.3	24.7	31.8	13.1	$(Al_2O_3)_{0.46}(MoO_{1.95})$	76.0 : 34.0	Th.4

Table 2: The proportion of APM / agar composite gel to $AlCl_3$ is given in the first column. The following columns report the elemental composition of $Al_xMo_yO_z$ phases in molybdenum, aluminium, oxygen and chlorine. The detailed formulae were determined from these data and then used to define the experimental proportions of $Al_xMo_yO_z$ to Al 50-P for each thermite.

From an experimental point of view, the $Al_xMo_yO_z$ phases and the Al 50-P powder are separately dispersed in hexane by applying intense sonic waves with a 400 W horn. The ultrasounds are continuously delivered at the maximum amplitude during 15 to 20 minutes. Finally, the two suspensions are mixed together by a 10 minutes additional sonication. In order to avoid the interactions of the thermite mixtures with the ambient atmosphere during the drying step, the hexane is extracted by evaporation under reduced pressure (T = 90°C). The thermite powders are kept away from the atmospheric moisture in a glass desiccator containing phosphorus pentoxide as desiccating agent.

2.2. Structural characterization of $Al_xMo_yO_z$ / Al nanothermites

$Al_xMo_yO_z$ thermites were characterized by SEM (the corresponding micrographs are not shown here). In the Th.1 material, the micron-sized MoO_3 particles are surrounded by the Al 50-P nanoparticles. In the Th.2, Th.3 and Th.4 samples the nanoparticles are homogeneously mixed and it is impossible to distinguish between the $Al_xMo_yO_z$ and the Al 50-P particles.

The specific area of $Al_xMo_yO_z$ thermites ($A_{Th.}$) was measured by nitrogen adsorption after a suitable process of desorption (T > 5 h, t = 150°C, helium flow). BET surface area was logically found to be equal to the weight balanced specific areas of each component:

$$S_{Th.} = \chi_{Al_xMo_yO_z} \times S_{Al_xMo_yO_z} + \chi_{Al50-P} \times S_{Al50-P}$$

This result indicates that there is neither physical nor chemical aggregation of the particles during the sonication (see § 2.1.).

2.3. Implementation of $Al_xMo_yO_z$ / Al powders

80 ± 1 mg samples of the $Al_xMo_yO_z$ / Al powders were pressed into cylindrical cohesive pellets using a mould designed for this purpose and a standard hydraulic press. No binding agent was used and a die load of 116 kg corresponding to a pressure of 557 MPa was applied to each material. The pellets were stuck with an epoxy resin on Duralumin discs used as supports during the experiments of time resolved cinematography.

3. Study of the reactivity of $Al_xMo_yO_z$ / Al based nanothermites

3.1. Classical characterization

The impact sensitivity of $Al_xMo_yO_z$ based thermites was investigated using a drop-weight system. This fall-hammer apparatus is equipped with a 5 kg mass which drops from a one meter

height, on a steel cell containing about 40 mm^3 of the tested sample. Concerning the thermites, the test is considered to be positive when black ashes are formed. A negative test leads to reflecting metallic sheets which burn in contact with an open flame. As shown below, the impact sensitivity of the $Al_xMo_yO_z$ / Al 50-P thermites is very low (**Table 3**). In fact, none of these materials react under the maximal stress.

A Julius-Peters measuring device was used to determine the sensitivity of the thermites to friction. A material laying down (about 10 mm^3) on a rough ceramic undergoes a friction by using a ceramic stick. The press intensity of this stick (expressed in Newton) is determined by the relative position of weights suspended from a lever. A test is assumed to be positive whenever an inflammation of the thermite is observed. The thermite containing only micron-sized molybdenum trioxide and the one with the MoO_3 richest $Al_xMo_yO_z$ phase (**Table 3**, Th.1 and Th.2 respectively) are the most sensitive to friction. On the other hand, the materials with the biggest alumina contents which contain the finest $Al_xMo_yO_z$ phases are less sensitive to friction (**Table 3**, Th.3 and Th.4). The nano-structuring of the $Al_xMo_yO_z$ phases makes the thermites more insensitive to friction.

The thermal decomposition of thermites was studied with a TGA / DSC apparatus using a 20 $K.min^{-1}$ heating rate from room temperature to 1773 K, in an argon flow. The decomposition of the $Al_xMo_yO_z$ based thermites under progressive heating occurs following a two exothermic steps mechanism:

- The first step is characterized by a low exothermic signal with a complex shape and a low onset temperature (**Table 3**).
- A strong exothermic signal is associated to the second step. It corresponds in fact to the combustion reaction of the thermite. As the temperature range of TGA / DSC apparatus was not wide enough, it was not possible to determine the energy released by this combustion (T_{max} = 1773 K).

As the onsets of the combustion of the Th.2, Th.3 and Th.4 samples are higher than the Th.1 onsets, it can be assumed that they are less sensitive to thermal stress.

Composition	Impact sensitivity (J)	Friction sensitivity (N)	Thermal sensitivity T onset (K)	
Th.1	> 49	212	741.4	1483.4
Th.2	> 49	212	798.6	1580.7
Th.3	> 49	282	813.0	1611.2
Th.4	> 49	> 353	807.7	1571.0

Table 3: Classical energetic characteristics of $Al_xMo_yO_z$ / Al 50-P based nanothermites.

3.2. Characterization by time resolved cinematography and spectroscopy

The time resolved cinematography (TRC) is an advanced method specifically devoted to the reactive characterization of energetic materials which was first described by Pantoya et al[7]. From an experimental point of view, the energetic material is ignited by a laser beam which is focused by the mean of a lens disposed on an optical bench. The ignition delay time is the duration between the laser impact on the energetic material and the beginning of its combustion. The ignition delay time (δ) can be correlated to the density of surface energy (activation energy E_a) necessary to initiate the material. To this purpose, it is necessary to know the effective power (P) delivered by the laser source as well as the diameter (Φ) of the laser beam:

$$E_a = \frac{4P\delta}{\pi\Phi^2}$$

The power of the focalized laser beam was measured with a calorimeter and was found to be equal to 9 W. The average diameter of the laser beam at the surface of the nanothermite pellet was determined by optical microscopy observations of the section of the burnt zone induced by the laser impact on a photographic film paper ($\Phi \approx 1.4$ mm). The combustion rate

(V_r) is measured by ultra fast cinematography using a Photron camera which can capture till 125,000 frames per second. The flame temperature (T_f) is measured by spectrometry.

Contrary to the classical analysis methods (see § 3.1), the time resolved cinematography allows to classify unambiguously the nanothermites according to their reactivity (**Table 4**). The $Al_xMo_yO_z$ based nanothermites have shorter ignition delay times than the micron-sized based MoO_3 thermite. Moreover, the ignition delay time is minimal for a intermediate alumina content. That corroborates that the ignition delay time is related to the structuring of the oxidative phase as well as to the amount of inert phase (alumina). The nano-structuring of the oxidative phase induces a strong increase of the combustion rate. The Th.2 nanothermite burns for instance sixty times faster than the Th.1 thermite. In the case of the $Al_xMo_yO_z$ based nanothermites, the combustion rate logically decreases when the alumina content becomes more important. It can be explained by the fact that alumina limits the mass transfer between reactive entities (MoO_u and Al). The more the thermites contain alumina, the lower are the combustion temperatures. Actually, the combustion temperature of a thermite does not depend on its particles size but on the chemical composition of the particles it is made off. The theoretical decomposition temperature of a MoO_3 / Al stoichiometric mixture is equal to 3253 K[8]. The experimentally measured value is lower ($T_{f/Th.1}$ = 2667 K) because the aluminium is in slight excess in comparison to the ideal stoichiometry (see §2.1). In addition, the alumina content of nano-sized aluminium is important (see §2.1). From a pyrotechnical point of view, the alumina is considered as an inert compound which does not chemically react but absorbs a part of the energy released by the thermite combustion. So, the presence of alumina results in a significant decrease of the flame temperature. The flame temperatures of the Th.2, Th.3 and Th.4 nanothermites are higher for these materials because the molybdenum is not only present at the + VI oxidation state corresponding to MoO_3 (see §1.4). The temperature decrease from the Th.2 to the Th.4 material is related to the alumina growing content.

Composition	Ignition delay time δ (ms)	Activation energy E_a ($J.cm^{-2}$)	Combustion rate V_r ($cm.s^{-1}$)	Combustion temperature T_f (K)
Th.1	17.8 ± 1.9	9.6 ± 1.0	1.7 ± 0.2	2667
Th.2	4.4 ± 1.4	2.3 ± 0.7	103.0 ± 10.6	3206
Th.3	2.8 ± 0.8	1.5 ± 0.5	59.8 ± 1.6	3131
Th.4	5.4 ± 0.6	2.9 ± 0.3	21.0 ± 4.2	2706

Table 4: Characterization by time resolved cinematography and spectroscopy of $Al_xMo_yO_z$ / Al 50-P based nanothermites.

4. Conclusions

The synthesis process described in this study allows the elaboration of $Al_xMo_yO_z$ nano-sized phases which contain alumina associated with molybdenum oxides MoO_u ($2 < u < 3$). This process consists to use agar as structuring agent of a molybdenum oxide precursor (APM). The corresponding materials are composite gels of agar and APM. The removal of agar and the APM conversion into molybdenum oxide are performed by a thermal oxidative treatment. The direct calcination of the composite gels leads to the formation of micron-sized molybdenum trioxide (MoO_3) particles. One the other hand, if the composite gels are impregnated with an AAT / Et_2O solution before calcination, the resulting $Al_xMo_yO_z$ phases are nano-sized.

The nanothermites elaborated by physical mix of these phases with nano-sized aluminium (Al 50-P) are very insensitive to mechanical and thermal stresses, but can easily be ignited by a convenient laser source. Their ignition delay times do not exceed a few milliseconds and their combustion rates are between twelve and sixty times faster than the combustion rate of thermite

composed of micron-sized MoO_3 particles. The energetic characteristics are tuned by adjusting the ratio CG : AAT in the synthesis process.

These promising characteristics allow considering these metastable interstitial composites (MICs) as potential components for insensitive weapon ignition systems.

Acknowledgments

The authors would like to thank J.P. Moeglin, E. Stechele and A. Boffy who conceived the laser device used to ignite the nanothermites, Y. Suma for the video sequences realization, U. Werner for the spectroscopic measurements and N. Chery who worked on the optimization of the synthesis of agar / APM composite gels. We are grateful to G. Pourroy and S. Joulié of the Institut de Physique et Chimie des Matériaux de Strasbourg (IPCMS / CNRS) for the TEM observations.

References

[1] M.L. Pantoya and J.J. Granier, Combustion Behavior of Highly Energetic Thermites: Nano versus Micron Composites, *Propellants, Explosives, Pyrotechnic*, **2005**, 30, 53-62.

[2] K.C. Walter, C.E. Aumann, R.D. Carpenter, E.H. O'Neill, and D.R. Pesiri, Energetic Materials Development at Technanogy Materials Development, *Materials Research Society Symposia Proceedings*, **2004**, 800, 27-37.

[3] T. Kawano, H. Imai, Characteristically shaped ZnO particles produced by periodic precipitation in organic gel media, *Journal of Crystal Growth*, **2005**, 283, 490-499.

[4] M. Comet, D. Spitzer, Des thermites classiques aux Composites Interstitiels Métastables, *Actualité Chimique*, **2006**, accepted 22.12.05. under press.

[5] A.L. Ramaswamy, P. Kaste, A "Nanovision" of the Physiochemical Phenomena Occurring in Nanoparticles of Aluminium, *Energetic Materials*, **2005**, 23, 1-25.

[6] D. Pesiri, C.E. Aumann, L. Bilger, D. Booth, R.D. Carpenter, R. Dye, E. O'Neill, D. Shelton, and K.C. Walter, Industrial Scale Nano-Aluminium Powder Manufacturing, *Journal of Pyrotechnics*, **2004**, 19, 19-31.

[7] J.J. Granier, M.L. Pantoya, Laser ignition of nanocomposite thermites, *Combustion and Flame*, **2004**, 138, 373-383.

[8] S.H. Fischer and M.C. Grubelich, Theoritical Energy Release of Thermites, Intermetallics, and Combustible Metals, *Proceedings of the 24th International Pyrotechnics Seminar*, Monterey, California, USA, 27-31 July, **1998**.